Simulation of Intracranial Acoustic Fields in Clinical Trials of Sonothrombolysis

Cecile Baron, Jean-François Aubry, Mickael Tanter, Stephen Meairs, Mathias Fink

Ultrasound in Med. & Biol., Vol. ■, No. ■, pp. 1–11, 2009

0301-5629/09/$–see front matter

ELSEVIER

doi:10.1016/j.ultrasmedbio.2008.11.014

● *Original contribution*

SIMULATION OF INTRACRANIAL ACOUSTIC FIELDS IN CLINICAL TRIALS OF SONOTHROMBOLYSIS

CECILE BARON,* JEAN-FRANÇOIS AUBRY,* MICKAEL TANTER,* STEPHEN MEAIRS,† and MATHIAS FINK*

*Laboratoire Ondes et Acoustique, University Paris 7, Paris, France; and †Department of Neurology, Universitätsklinikum Mannheim, University of Heidelberg, Mannheim, Germany

(*Received* 13 *March* 2008, *revised* 5 *November* 2008, *in final form* 14 *November* 2008)

Abstract—Two clinical trials have used ultrasound to improve tPA thrombolysis in patients with acute ischemic stroke. The Combined Lysis of Thrombus in Brain Ischemia Using Transcranial Ultrasound and Systemic tPA (CLOTBUST) trial reported accelerated recanalisation of the middle cerebral artery (MCA) in patients with symptoms of MCA infarction, which were monitored with 2-MHz transcranial Doppler. In CLOTBUST, there was no increased bleeding as evidenced by cranial computed tomography. The Transcranial Low-Frequency Ultrasound-Mediated Thrombolysis in Brain Ischemia (TRUMBI) trial, which employed magnetic resonance imaging (MRI) before and after tPA thrombolysis, was discontinued prematurely because of an increased number of secondary hemorrhages, possibly related to the use of low frequency 300-kHz ultrasound. The purpose of our work is to help identify possible mechanisms of intracerebral hemorrhage resulting from sonothrombolysis by applying a simulation tool that estimates the pressure levels in the human brain that are produced with different sonothrombolysis devices. A simulation software based on a finite difference time domain (FDTD) three-dimensional (3D) scheme was developed to predict acoustic pressures in the brain. This tool numerically models the wave propagation through the skull and reproduces both ultrasound protocols of CLOTBUST and TRUMBI for analysis of the distribution of acoustic pressure in the brain during stroke treatment. For the simulated TRUMBI trial, we analyzed both a "high" and "low" hypothesis according to published parameters (for high and low amplitude excitations). For these hypotheses, the mean peak rarefactional pressures in the brain were 0.26 ± 0.2 MPa (high hypothesis) and 0.06 ± 0.05 MPa (low hypothesis), with maximal local values as high as 1.2 MPa (high hypothesis) and 0.27 MPa (low hypothesis) for configurations modelled in this study. The peak rarefactional pressure was thus higher than the inertial acoustic cavitation threshold in the presence of a standing wave in large areas of the brain, even outside the targeted clot. For the simulated CLOTBUST trial, the maximum peak negative pressure was less than 0.07 MPa. This simulated pressure is below the threshold for both inertial and stable acoustic cavitation but likewise lower than any acoustic pressure that has been reported as sufficient for effective sonothrombolysis. Simulating the pressure field of ultrasound protocols for clinical trials of sonothrombolysis may help explain mechanisms of adverse effects. Such simulations could prove useful in the initial design and optimization of future protocols for this promising therapy of ischemic stroke. (E-mail: norabelic@yahoo.fr) **© 2009 World Federation for Ultrasound in Medicine & Biology.**

Key Words: **Stroke, Ultrasound, Sonothrombolysis, Numerical simulation, Safety.**

INTRODUCTION

Stroke is now the second leading cause of death in industrialized countries. The great majority of strokes are ischemic (85%). This is generally due to a blood clot, which occludes a cerebral artery and causes brain necrosis in the territory of the supplying vessel. The key point in the treatment of ischemic stroke is the rapidity of the reperfusion to avoid irreversible damage of brain tissue and sequelae for the patient (Caplan 1999). So far, intravenous recombinant tissue plasminogen activator (tPA) is the only effective and approved treatment available for acute ischemic stroke, despite controversial results concerning the balance between its established beneficial thrombolytic effect and its potential neurotoxicity (Benchenane et al. 2004).

Several *in vitro* and *in vivo* (animal models) studies have revealed that ultrasonic exposure of clots (with $I_{SPTA.3}$ ranging from 700 to 1750 mW/cm^2) accelerates the effect of fibrinolytic agents over a wide range of frequencies (from 20 kHz to 2 MHz) (Kudo 1989; Lauer et al. 1992; Kornowski et al. 1994; Francis et al. 1995;

Address correspondence to: Cecile Baron, Laboratoire Ondes et Acoustique, CNRS, ESPCI, University Paris 7, INSERM, 10, rue Vauquelin, 75005 Paris, France. E-mail: norabelic@yahoo.fr

Behrens et al. 1999; Alexandrov et al. 2004; Daffertshoffer et al. 2004). Mechanisms of ultrasound-accelerated tPA thrombolysis include reversible disaggregation of cross-linked fibrin fibers (Braaten et al. 1997), microcavity formation in the shallow layer of thrombus (Kondo et al. 1999) and increased uptake and penetration of tPA into clots (Francis et al. 1995). Cavitation, bubble formation in the rarefactional pressure zones, plays an important role in the production of such bioeffects (Blinc et al. 1993; Everbach and Francis 2000; Behrens et al. 2001; Meunier et al. 2007). Thermal effects may also contribute to ultrasound-assisted thrombolysis (Shaw et al. 2006)

Two clinical trials of sonothrombolysis for treatment of ischemic stroke have been reported. CLOTBUST (Combined Lysis of Thrombus in Brain Ischemia Using Transcranial Ultrasound and Systemic tPA) (Alexandrov et al. 2004) was a multicenter randomized clinical trial on 126 patients who had acute ischemic stroke due to occlusion of the middle cerebral artery (MCA). All patients were treated with intravenous tPA within 3 h after the onset of symptoms. Target patients received along with tPA, 2-MHz, pulsed wave transcranial Doppler monitoring for a duration of 2 h. A complete reperfusion or dramatic clinical recovery was observed for 49% of the patients in the target group (tPA + US) and for only 30% of the control group. No secondary effects linked with ultrasound exposure were identified.

Another clinical trial on sonothrombolysis, the TRUMBI trial (Transcranial Low-Frequency Ultrasound-Mediated Thrombolysis in Brain Ischemia), was stopped prematurely because of the occurrence of a higher number of intracerebral hemorrhages after tPA treatment combined with transcranial sonication at 300 kHz (Daffertshofer et al. 2005). Unlike the CLOTBUST study, rigorous MRI monitoring was performed in all patients and not just in those where control imaging after thrombolysis was warranted clinically. This led to detection of MRI evidence of hemorrhage in 93% of the target patients and 42% of the control patients in TRUMBI. Among these hemorrhages, all were classified as hemorrhagic transformation in the tPA only group versus 61% in the tPA plus ultrasound group. Five hemorrhages in the target group were symptomatic hemorrhages, possibly linked to ultrasound exposure.

The reasons for the different outcomes in these two clinical trials of sonothrombolysis are unclear. Indeed, experimental studies using animal models (Daffertshoffer et al. 2004) were unable to demonstrate harmful secondary effects of ultrasound insonification using TRUMBI parameters. One report has suggested that hemorrhages in TRUMBI were related to abnormal permeability of the human blood-brain barrier that was induced by wide-field low-frequency insonation (Reinhard et al. 2006). Wang and coworkers (Wang et al. 2008) hypothesize that in TRUMBI a pulse length of 765 mm combined with a very wide beam can cause overlap many times as the wave runs its course back and forth across the brain, reflecting off the skull. Therefore, the instantaneous intensity of ultrasound in the brain tissue may multiply constructively at some localized sites of brain tissue, resulting in MIs that are larger than the maximum limit set by the Food and Drug Administration (FDA). Q5

The purpose of our work is to better understand the brain pressure amplitude distribution involved in these studies through numerical simulations. This approach may allow localization of potential areas of acoustic cavitation and, thus, help explain mechanisms of adverse effects of sonothrombolysis.

MATERIALS AND METHODS

Ultrasound parameters from clinical studies of sonothrombolysis

All the pressure levels involved in the clinical studies (CLOTBUST or TRUMBI) have been deduced from data collected in various publications. Namely, peak negative pressure had to be deduced from the derated $I_{SPTA.3}$.

$$I_{SPTA.3} = P_-^2 / 2\rho c \quad (1)$$

ρ is the mass density and c is the ultrasound wave's velocity. The derating factor is fixed to 0.3 dB/cm-MHz and the derated intensities are noted with the index ''.3'' (AIUM/NEMA 1992). Due to the frequencies used in the clinical studies, the derated $I_{SPTA.3}$ has to be taken into account carefully in the CLOTBUST study whereas the value of $I_{SPTA.3}$ is very close to that of $I_{SPTA.3}$ in the TRUMBI protocol.

Assuming that the nonlinear effects are negligible in this configuration, we considered

$$P_{p2p} = 2P_- \quad (2)$$

P_{p2p} is the peak-to-peak acoustic pressure.

CLOTBUST study. The emitter was a 10 mm-diameter single element delivering a 2-MHz pulsed wave with duty cycle of 15% and short emission duration of 15 μs. The focusing was set in the ipsilateral hemisphere. The focal length depends on the targeted region: proximal (between 30 mm and 45 mm) or distal (more than 45 mm). At 45 mm away from the transducer, the derated spatial-peak time-averaged intensity, $I_{SPTA.3}$ was measured at 739 mW/cm^2 (Moehring et al. 2005) and a $I_{SPPA.3}$ of 4.9 W/cm^2. The corresponding pressure in water is, thus, equal to 0.385 MPa.

TRUMBI study. The diamond pattern transducer (50 mm diameter) emitted an unfocused pulsed ultrasound wave at 300 kHz modulated in frequency ($\pm$1.5 kHz) to

limit standing waves. The targeted zone was the contralateral brain hemisphere corresponding to a distance around 100 mm.

The emission parameters reported in (Daffertshofer et al. 2005) include a 5% duty cycle (corresponding to an emission duration of 500 μs) and a spatial-peak time-average intensity ($I_{SPTA.3}$) of 700 mW/cm^2 in water with a pulse repetition frequency of 100 Hz.

Taking into account the duty cycle, the spatial-peak pulse-average intensity ($I_{SPPA.3}$) was 14 W/cm^2, corresponding to a mechanical index (MI) in water of 1.18. However, the authors claim that the mechanical index was less than 0.2. Wang (2007) recently estimated the MI used in the TRUMBI study and concluded that the value given in (Daffertshofer et al. 2005) was wrong: the MI was 1.18 and the pressure was higher than the one expected by the authors of the TRUMBI study. However, a closer look at the description of the emission parameters given in (Daffertshofer et al. 2005) could be interpreted in another way: the 5% duty cycle has been added in order to ''further reduce thermal effects'' and was, thus, not taken into account in the evaluation of the 700 mW/cm^2 $I_{SPTA.3}$ in water, so that technically speaking, it corresponds to an $I_{SPPA.3}$ of 0.7 W/cm^2. This corresponds to the back-calculation of a mechanical index of 0.25.

To summarize, data given in (Daffertshofer et al. 2005) are not coherent: either the given MI is equal to 1.18 instead of 0.2. Since it is unclear which interpretation of the published data is correct, both parameters will be evaluated in this study, according to two separated hypothesis.

High hypothesis. The MI is equal to 1.18. It corresponds to an $I_{SPPA.3}$ of 14 W/cm^2 . This hypothesis is supported by Wang et al (2007) and corresponds to the published $I_{SPTA.3}$ (Daffertshofer et al 2005). The corresponding pressure in water is, thus, equal to 0.65 MPa.

Low hypothesis. The MI is equal to 0.2. It corresponds to an $I_{SPPA.3}$ of 0.7 W/cm^2. This hypothesis is supported by the designers of the TRUMBI device and corresponds to the published MI value (Daffertshofer et al 2005). The corresponding pressure in water is, thus, equal to 0.15 MPa.

A frequency modulation was used in the TRUMBI study to avoid standing waves: 300 ± 1.5 kHz but no reference to the exact frequency modulation was given. Different frequency modulation options have, thus, been tested: ramp or sinusoidal modulation. Furthermore, in order to study the influence of the frequency modulation, various frequency ranges have been modelled (300 kHz; 300 ± 1.5 kHz; 300 ± 15 kHz; 300 ± 150 kHz).

Ultrasonic parameters of both CLOTBUST and TRUMBI studies are summarized in Table 1.

The mechanical index (MI)

In order to evaluate the likelihood of cavitation-related biological effects, the most relevant indicator was established to be the mechanical index (MI) (Apfel and Holland 1991). Indeed acoustic cavitation activity occurs in areas of rarefactional pressure and depends on the ultrasound frequency. The MI is defined as follows:

$$\mathrm{MI}=\frac{P_-}{\sqrt{f}} \tag{3}$$

with P_- the in situ peak rarefactional pressure in megapascal and f the ultrasound center frequency in megahertz.

In this study, as the simulation is taking into account the absorption in the tissues, the computed pressure corresponds to the in situ peak rarefactional pressure P_-. Equation 3, thus, enables to directly calculate the simulated MI.

To avoid adverse biologic effects related to acoustic cavitation, the FDA (FDA–510K Norm 1992) imposes the diagnostic devices to ensure a MI less than 1.9 (Dalecki 2004).

No adverse biologic effect induced by ultrasound alone on mammals has been recorded for MI $<$ 0.3 (AIUM/NEMA 1992). Nevertheless, this threshold may be lowered in the presence of tPA and clot and in a standing wave field.

Importantly, this definition of MI is only valid for single cycle pulses. As in previous publications (Daffertshofer et al. 2005; Wang et al. 2008), it will be used later in this article to analyse previous results. Significant work has been done on the influence of pulse duration and pulse repetition frequency on the safety of ultrasound-induced lung hemorrhage (O'Brien Jr 2007). Church and O'Brien Jr. introduced recently a modified MI taking into account the pulse length (Church and O'Brien Jr 2007). Basically, the threshold for cavitation decreases with pulse length and reaches a plateau for 10 cycles: the modified MI is three times higher than the classical one in water. All the MIs given in this article refer to conventional calculations (for one cycle pulses). As all pulses have much more than 10 cycles, such MIs do not reflect the exact biologic effects of ultrasound but only serve as reference for the readers in addition to the pressure levels.

The skull acoustical model

From high resolution computed tomography (CT) images, a three-dimensional (3D) portion of the skull is reconstructed. CT images were acquired with a GE Genesis CT scanner (3 mm slice thickness, 1 mm between slices, slice resolution: 0.69 mm × 0.69 mm) at the Curie Institute Hospital (Paris, France). The Curie Institute institutional review board approved the imaging protocol and data was anonymized before transmission to the

Table 1Parameters for the two trials

	CLOTBUST	TRUMBI
Number of patients	126	26
Transducer diameter (mm)	10	50
Focused/unfocused	yes	no
Distance of the target (mm)	Proximal (30-45) Distal (>45)	100
Frequency (MHz)	2	0.3
Emission duration (μs)	15	500
Pulse repetition frequency (MHz)	0.1	0.0001
I_{SPPA} (W/cm^2)	4.9	14 (high hypothesis) 0.7 (low hypothesis)
Peak negative pressure in water	0.385	0.65 (high hypothesis) 0.15 (low hypothesis)

Q14 CLOTBUST = Combined Lysis of Thrombus in Brain Ischemia Using Transcranial Ultrasound and Systemic tPA; TRUMBI = Transcranial Low-Frequency Ultrasound-Mediated Thrombolysis in Brain Ischemia.

Laboratoire Ondes et Acoustique. All measurements and simulations were performed on one female skull. Patient data protection regulations for this study do not allow disclosure of ethnic group or age. As previously described in (Aubry et al. 2003), the acoustical properties of the skull are then deduced from the raw CT data.

The brain acoustical model

The brain is considered as soft tissue with an acoustical behavior close to that of water (Wells 1977):

$$\rho_{\text{brain}} = 1000\text{kg/m}^3;\ c_{\text{brain}} = 1500\text{m/s} \qquad (4)$$

The brain is an absorbing medium, the absorption coefficient depends on the ultrasound frequency and was set to (Goss et al. 1978).

$$\text{abs}_{\text{brain}} = 0.5\text{dB/cm/MHz} \qquad (5)$$

Thus, in our simulations the brain is modelled by a homogeneous absorbing medium.

Simulation code

Three-dimensional (3D) finite simulations have been performed in order to evaluate pressure field distributions and pressure levels in the brain. Simulations were performed with a C++ finite differences program developed Q9 at the Laboratoire Ondes et Acoustique (UMR CNRS 7587, Paris, France). The scalar heterogeneous wave equation with loss absorption (eqn 6) was discretized with a second order in space and second-order centered in time scheme. A fourth order approximation Higdon absorption boundary (Higdon 1991) condition was used on computation volume borders to avoid unphysical reflections (reflections are typically 40 dB lower than the incident wave field over a wide range of incidence angles).

$$\left(1+\tau(\vec{r})\frac{\partial}{\partial t}\bullet\right)\left[\rho(\vec{r})\,\nabla\bullet\left(\frac{1}{\rho(\vec{r})}\nabla\, p\,(\vec{r},t)\right)\times\right]-\frac{1}{c(\vec{r})^2}\frac{\partial^2 p\,(\vec{r},t)}{\partial\, t^2}=S(\vec{r},t) \qquad (6)$$

where $c(\vec{r})$is the speed of sound, $\rho(\vec{r})$ the density and $\tau(\vec{r})$ the absorption coefficient in the medium either in the skull bone or in the brain. The pressure field p and the source term S depend on both space and time.

Simulations were conducted at 2-MHz and 300-kHz central frequency. The simulation grid was set to one tenth of a wavelength. In order to meet the Von Neumann stability criteria (Press et al. 1992), the temporal step is given by $\Delta t < \frac{\Delta x}{\max_{\vec{r}}(c_0(\vec{r}))\sqrt{3}}$, where Δx is the spatial step of the grid. An example of the 3D pressure field in the region of interest located in front of the transducer is given on Fig. 1. One can see the appearance of vibration nodes and antinodes in the 3D wave field distribution. For sake of clarity, only two-dimensional (2D) views will be displayed in the results. In both studies, we assumed that the clinicians located the transducers optimally, perpendicularly to the temporal window. Such a configuration was reproduced at best in the simulation process.

Definition of the targeted area

Each clinical study had its own procedure to target the clot once it was located.

Trumbi. The transducer was positioned on the temporal bone window on the contralateral side of the head with a clot-probe distance around 100 mm (Daffertshofer et al. 2005).

Clotbust. The transducer was positioned on the temporal bone window ipsilateral to the clot. Typically, the clot-probe distance was around 45 mm (Alexandrov et al. 2004).

According to each set-up, the location of the targeted region has been estimated in respect to the location of the probe. Even though no model of clot has been introduced in the simulations, pressure levels obtained in the expected location of a clot were analyzed for each study. Such regions-of-interest (1 cm × 1 cm × 1 cm) will be later referred to as ''expected location of the clot''. Parameters described in this section are summarized in Table 1.

Cavitation threshold

In order to determine in which areas of the brain inertial cavitation might occur, the pressure field simulated in the brain has been mapped. The areas where the pressure

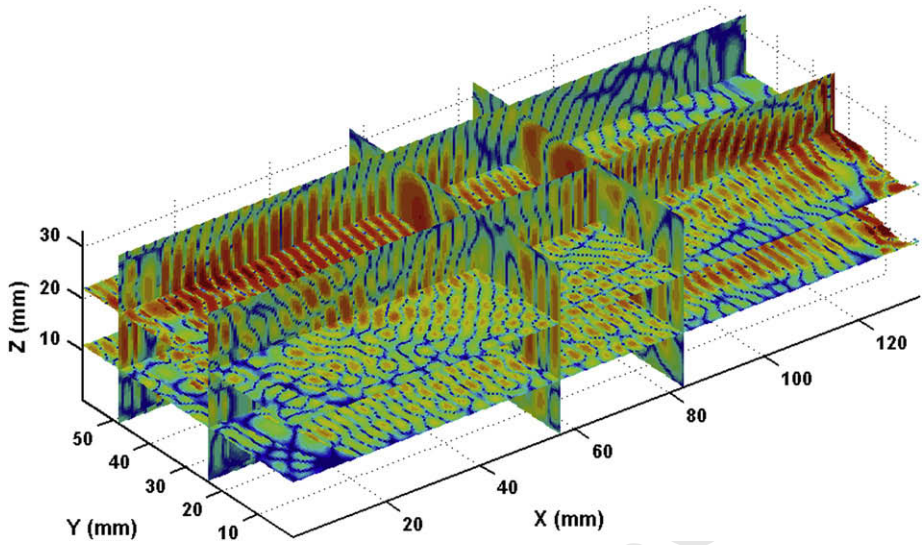

Fig. 1. Three-dimensional simulation of the acoustic field after propagation through the skull bone (in a dB scale with a 60 dB dynamic). The transducer is located on the right side of the image.

went beyond the threshold for inertial acoustic cavitation in a standing wave field have been plotted. The inertial acoustic cavitation threshold applied to our analysis was derived from (Azuma et al. 2005). In Azuma's study the acoustic cavitation threshold was measured in degassed water, in a standing wave field established inside a human skull, at 617-kHz frequency. The back-calculated peak rarefactional pressure was 0.27 MPa. By considering that the cavitation threshold increases as the square root of the frequency, the corresponding threshold at 300 kHz is equal to 0.19 MPa. It is important to note here that the cavitation threshold in a standing wave field is much smaller than the threshold in a progressive wave field. This is mainly due to the fact that nanobubbles can be trapped in antinodes and create bigger bubbles by coalescing (Azuma et al. 2005). Those microbubbles inertially collapse as soon as they reach their resonant size.

RESULTS

The TRUMBI study

Several points are crucial in analyzing the interaction between the biologic medium and the ultrasound field: the location and the amplitude of the peak rarefactional pressure and the possibility of standing waves formation.

Peak rarefactional pressure. In the whole area of the brain in front of the transducer, the mean peak rarefactional pressure is equal to 0.26 ± 0.2 MPa in the case of the high hypothesis and 0.06 ± 0.05 MPa in the case of the low hypothesis.

Table 2 summarizes the simulated pressure levels at the expected location of the clot and the maximum pressure levels achieved in the brain (on the so-called ''hot spot'') with the corresponding MI: the maximum peak rarefactional pressure in the brain is equal to 1.2 MPa for the high hypothesis and 0.27 MPa for the low hypothesis. At the expected location of the clot, the maximum peak rarefactional pressure is equal to 1 MPa for the high hypothesis and 0.22 MPa for the low hypothesis.

The location of the corresponding maximum pressure levels achieved in the brain can be seen in Fig. 2 (black dots). The location of these ''hot spots'' is highly dependent on the skull shape and on the position of the probe. The pressure field distribution in the brain for two different locations of the probe has been represented:

Table 2Simulation results for the TRUMBI set-up

	Left temporal window (//skull)	Right temporal window (// skull)
Maximum peak rarefactional pressure (MPa) High hypothesis/low hypothesis	1.2/0.27	1.1/0.25
MI_{max} High hypothesis/low hypothesis	2.2/0.49	2/0.45
Pressure at the expected location of the clot (MPa) High hypothesis/low hypothesis	1/0.22	0.8/0.18
MI_{clot} High hypothesis/low hypothesis	1.8/0.40	1.5/0.33

TRUMBI = Transcranial Low-Frequency Ultrasound-Mediated Thrombolysis in Brain Ischemia.

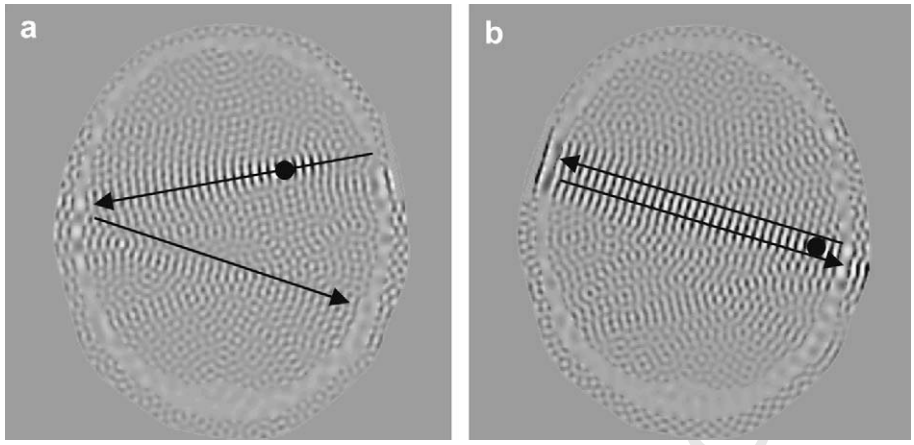

Fig. 2. Maximum peak rarefactional pressure (black spot) location and shape of the ultrasound field through (a) the right and (b) the left temporal windows.

probe located on the right temporal window (Fig. 2a) and on the left temporal window (Fig. 2b). The maximum peak rarefactional pressure is not located in the same area: between the emitter and the clot for the right window configuration and near the bone at the opposite side from the emitter for the left window configuration. Moreover, in Fig. 2a, the acoustic beam is reflected with an angle whereas in Fig. 2b the reflected wave travels parallel to the incident wave yielding to completely different pressure field distribution in the brain. In the latter case, a standing wave is likely to occur all the way in front of the transducer.

Standing waves. In order to have a closer look at potential standing wave formation, the acoustic pressure is presented as a function of time in Fig. 3 for our high hypothesis. In the case of the low hypothesis, the patterns are identical and only the pressure amplitudes differ. It corresponds to the configuration with the transducer located on the right temporal window. Each plot represents the pressure recorded at the location of the maximum pressure amplitude observed in the brain (a,''hot spot'') and at the expected location of the clot (b,''clot''). The distance of the ''hot spot'' from the emitter surface is 65 mm. The distance of the clot (targeted region) from the emitter surface is equal to 100 mm. One can see that the amplitude is varying with time, indicating interferences between direct waves and waves reflected on the contralateral skull.

Cavitation. Figure 4 represents in grey the areas where the pressure went beyond the threshold for inertial cavitation in a standing wave. The inertial acoustic cavitation threshold applied to our analysis was set to 0.19 MPa (derived from [Azuma et al. 2005]). During sonication, each time the simulated pressure levels went beyond the cavitation threshold, the corresponding pixel was definitely turned to from a black pixel to a grey one.

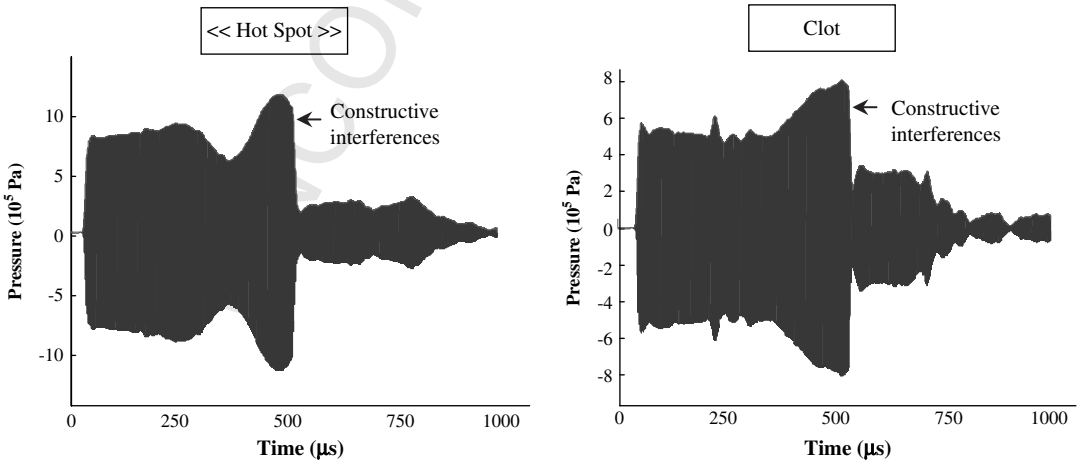

Fig. 3. Evolution of the acoustic pressure waveform as a function of time for one emission burst of 500 μs for two locations: at the maximum pressure amplitude location (left) and at the expected location of the clot (right).

The zone where the acoustic cavitation is liable to take place is not confined to the clot for both the low hypothesis (Fig. 4a) and the high hypothesis (Fig. 4b): such areas exist in tissues located in front of the transducer all along the brain. This observation may be related to the occurrence of atypical hemorrhages outside the targeted region.

Frequency modulation. Different frequency modulation options have been tested (Fig. 5) in order to take into account the frequency modulation used in the TRUMBI study. Areas where the acoustic pressure is higher than 0.19 MPa (Azuma et al. 2005) are displayed in grey color. Figure 5a is the reference, without modulation. Different frequency modulation options have been tested: ramp (left: Fig 5b, d and f) or sinusoidal modulation (right: Fig. 5c, e and g). Furthermore, in order to study the influence of the frequency modulation, various frequency ranges have been modelled (300 ± 1.5 kHz [Fig. 5b and c]; 300 ± 15 kHz [Fig. 5d and e]; 300 ± 150 kHz [Fig. 5f and 5g]). One can see that whatever the modulation, when frequency is shifted, the locations of the maximum pressure amplitude are shifted: nanobubbles are not trapped at the same location for a long time anymore but the pressure levels remains higher than 0.19 MPa in all cases.

The CLOTBUST study

The maximum peak negative pressure recorded in the simulation is equal to 0.07 MPa in the whole brain. The MI in the brain is thus less than 0.05. At the location of the maximum peak negative pressure (hot spot), the pressure is not affected by standing waves: the pressure reaches a plateau at 0.07 MPa during all the duration of the burst and vanishes at the end of the burst.

At the expected location of the clot, the peak negative pressure is 0.05 MPa, without any standing wave pattern. Standing waves are confined in the vicinity of the contralateral skull, within a 1 cm band. Nevertheless, in the standing wave area, the pressure field is one order of magnitude smaller than the hot spot. The main values of maximum peak negative pressure concerning both studies are summarized in Table 3.

DISCUSSION

For the CLOTBUST study, the simulated maximum negative peak pressure is 0.07 MPa: the simulated MI in the brain is less than 0.05. In fact, the pressure is so low after attenuation of the skull bone that it has been questioned whether any thrombolytic effect at all can be expected (Pfaffenberger et al. 2005). According to several *in vitro* studies (Blinc et al. 1993; Everbach and Francis 2000; Behrens et al. 2001; Meunier et al. 2007), stable acoustic cavitation seems to be the key process of low-frequency sonothrombolysis. As underlined by Vykhodtseva and colleagues (Vykhodtseva et al. 1995), it is very difficult to measure the stable and inertial cavitation thresholds in living tissues because they depend on numerous parameters: propagation medium, ultrasound frequency, duty cycle, pulse duration and standing wave. In a recent paper (Datta et al. 2006), Datta and colleagues demonstrated the sensitivity of cavitation thresholds to the medium. The likelihood of cavitational effects is higher when the ultrasound field is applied to plasma containing tPA and a clot, than when it is applied to plasma alone (Table 4). According to all experimental measurements of cavitation thresholds in tissues published in the literature, our simulations show that stable cavitation is not likely to occur in the brain with the CLOTBUST acoustical setup. Stable cavitation cannot explain the efficiency of the CLOTBUST approach. Nevertheless, there is little evidence that cavitation plays

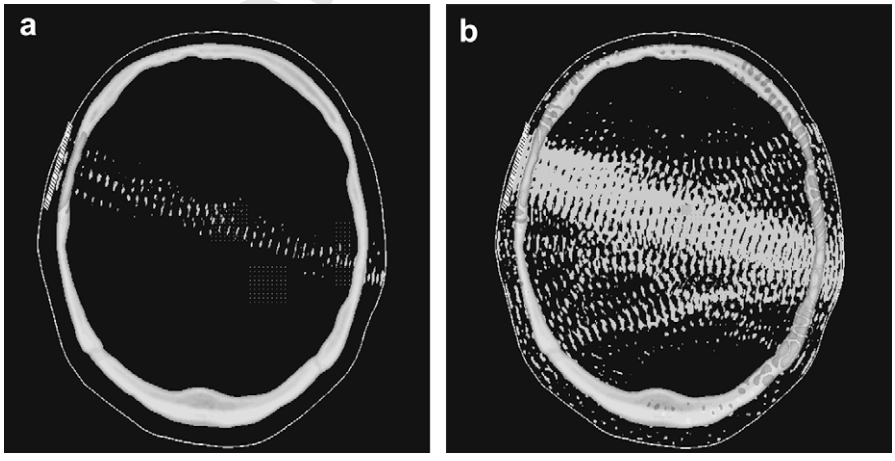

Fig. 4. Two-dimensional representation of the cavitation area (in grey) through one insonation for a 50 mm-emitter and with frequency modulation of the signal (ramp ± 1.5 kHz). (a) Low hypothesis. (b) High hypothesis.

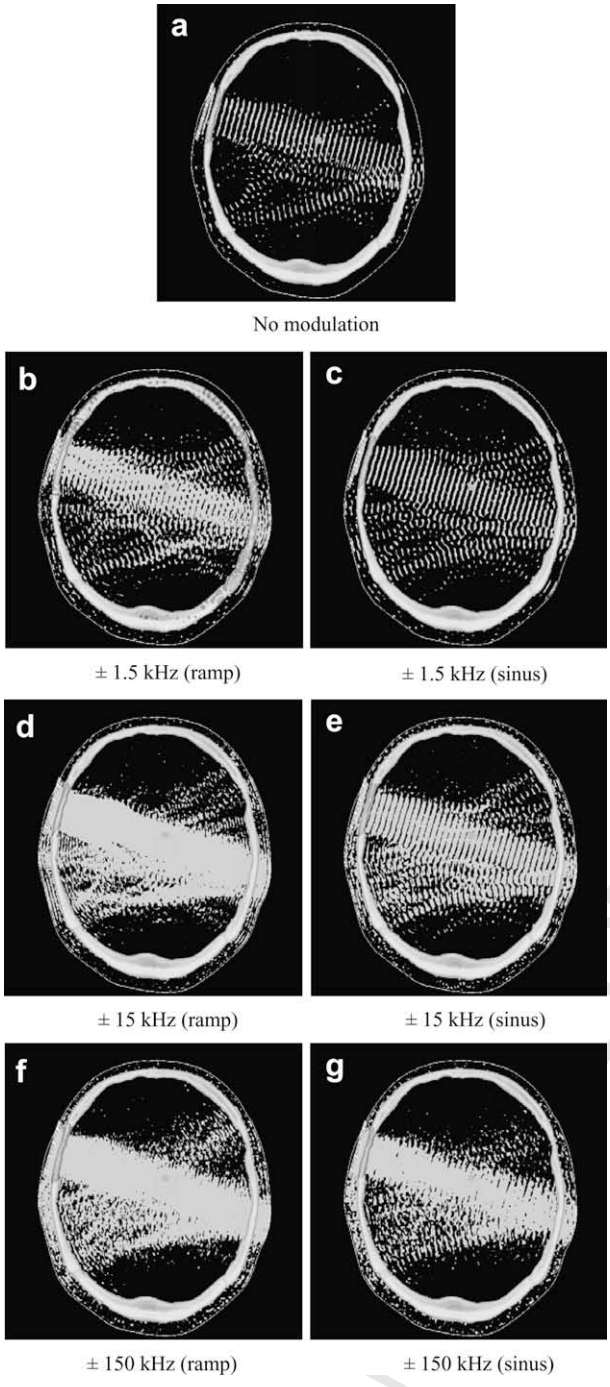

Fig. 5. Comparison of pressure repartition in different cases of frequency modulation.

such an important role *in vivo* and one should be cautious when extrapolating *in vitro* results to the clinical situation.

Several reports have hypothesized that high pressure amplitudes were used in the TRUMBI study (Azuma et al. 2005; Wang et al. 2008). Such reasoning was correct regarding the TRUMBI acoustical data available: MI and I_{SPTA} given in (Daffertshofer et al. 2005) where not compatible. Considering that the MI was not equal to 0.2 but that $I_{SPTA.3}$ was truly equal to 700 mW/cm^2 yielded high pressure levels generated in water (high hypothesis). In this article, a new analysis of the TRUMBI acoustical data has been proposed. We hypothesized a misspelling: $I_{SPTA.3}$ is not equal to 700 mW/cm^2 but $I_{SPPA.3}$ is. In that case, the MI meets 0.2. Such a low hypothesis is highly plausible. Q10

Whatever the pressure level, as first highlighted by Azuma (2005) the simulations performed in this article confirmed the possibility of standing wave formation when using the TRUMBI set-up on a human skull. Moreover, pressure field distributions in the brain could be plotted (Fig. 2). Standing waves are likely to occur not only near the bone (Fig. 2.a) (Azuma et al. 2005) but also all along the way in front of the transducer (Fig. 2b). As the emission duration in the TRUMBI protocol (500 μs) corresponds to several crossings of the brain, the ultrasound wave is reflected more than four times in the brain so that complex pressure fields can be obtained in the brain (Fig. 2). These pressure fields are highly dependent on the position of the transducer: the transducer was positioned at best perpendicularly to the bone for both left and right bone window configurations (Fig. 2a and b), as was performed clinically by the physician for each study. Even though human skulls are almost symmetrical, the pressure fields differ significantly, most probably due to slightly different angles between the probe and the skull. Interestingly, these figures highlight two remarkable different phenomena that are likely to occur in the brain during TRUMBI sonication.

Figure 2a. The plane wave emitted by the transducer has been focused towards the hot spot because of a lens effect induced by the shape of the skull: right after crossing the skull, the wave front is no longer planar, but cylindrical. Figure 6 highlights that in this configuration the maximum peak rarefactional pressure is precisely in the area where the atypical secondary hemorrhage occurred for the pathologic case reported in (Daffertshofer et al. 2005)

Figure 2b. The wave is reflected perpendicularly to the skull interface located at the opposite side the transducer, yielding to a standing wave pattern all the way in front of the transducer.

The skull bone is usually considered as a barrier for ultrasonic waves. Simulating the pressure fields generated by the TRUMBI set-up highlights a particular property of the skull: at low frequency, absorption is weak in the bone and in the brain, so that the skull potentially acts as a surpressure generator by either creating an acoustical lens (Fig. 2a) or acting as a resonator (Fig. 2b). These two examples are not exhaustive and other ways to generate hot spots in the brain can be envisioned: any constructive interference due to reflections on any part of the skull

Table 3Simulation results for CLOTBUST and TRUMBI set-ups

	CLOTBUST	TRUMBI (high hypothesis)	TRUMBI (low hypothesis)
Frequency	2 MHz	300 kHz	300 kHz
$I_{SPTA.3}$	700 mW/cm^2	700 mW/cm^2	35 mW/cm^2
Expected pressure in water	0.385 MPa	0.65 MPa	0.15 MP
Simulated maximum pressure in the brain	0.07 MPa	1.2 MPa	0.27 MPa

Q18 CLOTBUST = Combined Lysis of Thrombus in Brain Ischemia Using Transcranial Ultrasound and Systemic tPA; TRUMBI = Transcranial Low-Frequency Ultrasound-Mediated Thrombolysis in Brain Ischemia.

bone, like the orbital shelf or the anterior clinoid. The curvature of the skull plays an important role and may explain the discrepancy between the results of this study and the previous ones carried out *in vitro* or on animal models (Daffertshoffer et al. 2004).

Simulations demonstrate that due to the complex skull geometry and due to the length of the emission (500 μs), standing waves are likely to occur at the targeted location and outside the targeted location with pressure levels higher than 0.27 MPa (low hypothesis). On the contrary CLOTBUST simulations show that standing waves are confined to a 1cm band close to the contralateral skull with pressure levels 10 times lower than in the targeted location.

Q11 E-simulations could thus, explain the atypical secondary hemorrhages observed in the TRUMBI study for two reasons: the possibility of inertial cavitation in a large area of the brain is demonstrated in Fig. 4 but possible tPA extravasation might also occur. A recent paper (Reinhard et al. 2006) points out the abnormal permeability of the human blood-brain barrier (BBB) which can be induced by wide-field low-frequency insonation. The observed excessive bleeding rate with low-frequency sonothrombolysis might thus be attributable to primary BBB disruption by ultrasound. (Hynynen et al. 2006) evaluated the threshold for BBB disruption to 0.4 MPa, using 260-kHz focused ultrasound bursts and ultrasound contrast agent. This threshold is far below the maximum peak pressure amplitude simulated in the brain for the TRUMBI set-up with the high hypothesis and on the order of magnitude of the one simulated with the low hypothesis. Ultrasound could, thus, induce BBB opening in areas remote from the brain infarction so that tPA could diffuse in the brain parenchyma. As tPA is a known neurotoxic agent which can induce hemorrhages (Benchenane et al. 2004; Kaur et al. 2004), this might also explain the occurrence of secondary hemorrhages in TRUMBI.

Table 4Acoustic cavitation thresholds from (Azuma et al. 2005) and (Datta et al. 2006)

	Frequency (MHz)	Peak rarefactional pressure for cavitation (MPa)	MI
Q19			
(Azuma et al. 2005, inertial cavitation)			
Q20 Degassed water and skull	0.617	0.275	0.35
(Datta et al. 2006, inertial cavitation)			
Degassed water	0.12	>0.65	>1.88
Plasma alone	0.12	0.50	1.44
Plasma + tPA	0.12	0.47	1.36
Plasma + tPA + clot	0.12	0.27	0.78
(Datta et al. 2006, stable cavitation)			
Degassed water	0.12	>0.65	>1.88
Plasma alone	0.12	0.39	1.13
Plasma + tPA	0.12	0.34	0.98
Plasma + tPA + clot	0.12	0.2	0.58

One of the main differences between the clinical trials studied in this article is the ultrasound frequency. In the CLOTBUST trial, the frequency is seven times higher than in the TRUMBI trial, thus, the attenuation through the skull is much higher and explains mostly the difference in the pressure level. Sonothrombolysis devices are often characterized by the value of their I_{SPTA} in the absence of skull bone. Nevertheless, even though both studies claimed to have the same $I_{SPTA.3}$ (739 mW/cm^2 for CLOTBUST and 700 mW/cm^2 for TRUMBI), the simulated maximum pressure levels in the brain are significantly different: 0.07 MPa for CLOTBUST and 1.2 MPa (high hypothesis) or 0.27 MPa (low hypothesis). Basically, the skull attenuation is eight times lower in TRUMBI compared with CLOTBUST. In order to evaluate the safety and the efficiency of sonothrombolysis systems, the mean $I_{SPTA.3}$ (or mean peak negative pressure) expected in the brain appears to be more relevant than $I_{SPTA.3}$ value (or mean peak negative pressure) in water. We have shown that such pressure levels can be estimated with finite differences simulations. Moreover, simulation could be of value for optimizing the efficacy and the safety of new sonothrombolytic devices. For example, in order to reduce standing waves Daffertshoffer et al. (2005) proposed to apply a 0.5% frequency modulation. Our simulations have shown, however, that this approach would was not be sufficient to significantly reduce standing waves. Other strategies might include:

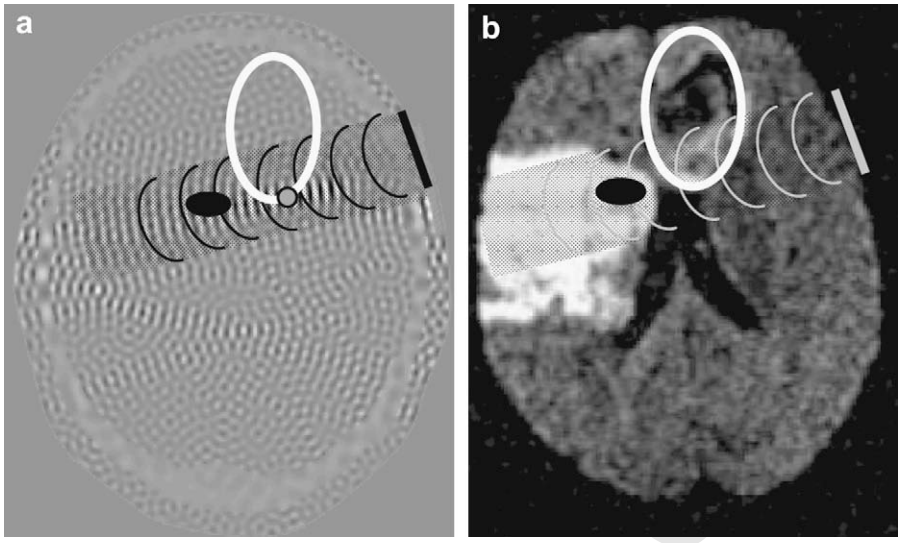

Fig. 6. Localization of the targeted clot (black spot) and of the peak rarefactional pressure (grey spot) with respect to the secondary hemorrhage location (white circle). Comparison between simulation results (left figure) and data from (Daffertshoffer et al. 2005) Fig. 3 (right figure).

(1) increasing the frequency modulation range (as tested in this article); (2) using random signal modulation; (3) using a higher frequency to decrease the interferences as absorption in the brain will be higher; and (4) shortening the emission duration in order to avoid the constructive interferences between a reflected wave and the emitted one. All these strategies could first be tested numerically.

CONCLUSION

Our simulation results of CLOTBUST acoustic parameters estimate the maximum peak negative pressure in the brain to be 0.07 MPa. Even though stable cavitation has been demonstrated *in vitro* to play a major role in ultrasonically enhanced thrombolysis, it is not likely to occur in CLOTBUST. A new and likely hypothesis (so-called low hypothesis) concerning the acoustical parameters used in the TRUMBI study has been introduced in this article for which the peak negative pressure is significantly lower than mentioned in previous studies (so-called high hypothesis). However, whatever the hypothesis, atypical secondary hemorrhages observed in the TRUMBI study can be explained: the pressure is well above (high hypothesis) or slightly above (low hypothesis) the inertial cavitation threshold for standing wave outside the targeted region and pressure levels can induce BBB opening, putting the brain at risk for tPA extravasations. In order to ensure the efficacy and safety of the sonothrombolysis treatment, the critical issue is to identify the optimum combination between frequency, intensity and waveform to perform the safest and the most efficient treatment. Numerical simulations provide a unique opportunity to explore different hypotheses and evaluate the pressure levels inside the brain. They should be of help in adjusting pressure levels for safely applying the benefits of ultrasound exposure in stroke treatment.

Acknowledgments—The authors wish to thank Ulrich Herken and Al Kyle for fruitful discussion.

REFERENCES

AIUM/NEMA. Standard for real-time display of thermal and mechanical acoustic output indices on diagnostic ultrasound equipment. Laurel, MD: AIUM Publication; 1992.

Alexandrov AV, Molina CA, Grotta JC, Garami Z, Ford SR, Alvarez-Sabin J, Montaner J, Saqqur M, Demchuk AM, Moyé LA, Hill MD, Wojner AW. Ultrasound-enhanced systemic thrombolysis for acute ischemic stroke. N Engl J Med 351:2170–2178.

Apfel RE, Holland CK. Gauging the likelihood of cavitation from short-pulse, low-duty cycle diagnostic ultrasound. Ultrasound Med Biol 1991;17:179–185.

Aubry J-F, Tanter M, Pernot M, Thomas J-L, Fink M. Experimental demonstration of noninvasive transskull adaptive focusing based on prior computed tomography scans. J Acoust Soc Am 2003;113: 84–93.

Azuma T, Kawabata K-I, Umemura S-I, Ogihara M, Kubota J, Sasaki A, Furuhata H. Bubble generation by standing wave in water surrounded by cranium with transcranial ultrasonic beam. Jpn Soc Appl Phys 2005;44:4625–4630.

Behrens S, Daffertshofer M, Spiegel D, Hennerici MG. Low-frequency, low-intensity ultrasound accelerates thrombolysis through the skull. Ultrasound Med Biol 1999;25:269–273.

Behrens S, Spengos K, Daffertshofer M, Schroeck H, Dempfle CE, Hennerici MG. Transcranial ultrasound-improved thrombolysis: Diagnostic versus therapeutic ultrasound. Ultrasound Med Biol 2001;27:1683–1689.

Benchenane K, Lopez-Atalaya JP, Fernandez-Monreal M, Touzani O, Vivien D. Equivocal roles of tissue-plasminogen activator in stroke-induced injury. Trends Neurosci 2004;27:155–160.

Blinc A, Francis CW, Trudnowski JL, Carstensen EL. Characterization of ultrasound-potentiated fibrinolysis *in vitro*. Blood 1993;18: 2636–2643.

Braaten JV, Goss RA, Francis CW. Ultrasound reversibility disaggregates fibrin fibers. Thromb Haemost 1997;78:1063–1068.

Caplan LR. Hemmorrhage into embolic brain infarcts. Pharmacotherapy 1999;19:125–127.

Church CC, O'Brien WD Jr. Evaluation of the threshold for lung hemorrhage by diagnosis ultrasound and a proposed new safety index. Ultrasound Med Biol 2007;33:810–818.

Daffertshofer M, Gass A, Ringleb P, Sitzer M, Sliwka U, Els T, Sedlaczek O, Koroshetz WJ, Hennerici MG. Transcranial low-frequency ultrasound-mediated thrombolysis in brain ischemia. Increased risk of hemorrhage with combined ultrasound and tissue plasminogen activator. Results of a phase II clinical trial. Stroke 2005;36:1441–1446.

Daffertshoffer M, Huang Z, Fatar M, Popolo M, Schroeck H, Kuschinsky W, Moskowitz MA, Hennerici MG. Efficacy of sonothrombolysis in a rat model of embolic ischemic stroke. Neurosci Lett 2004;361:115–119.

Dalecki D. Mechanical bioeffects of ultrasound. Ann Rev Biomed Eng 2004;6:229–248.

Datta S, Coussios C-C, McAdory LE, Tan J, Porter T, De Courten-Myers G, Holland CK. Correlation of cavitation with ultrasound enhancement of thrombolysis. Ultrasound Med Biol 2006;32:1257–1267.

Everbach EC, Francis CW. Cavitational mechanisms in ultrasound-accelerated thrombolysis at 1 MHz. Ultrasound Med Biol 2000;26:1153–1160.

Francis CW, Blinc A, Lee S, Cox C. Ultrasound accelerates transport of recombinant tissue plasminogen activator into clots. Ultrasound Med Biol 1995;21:419–424.

Goss SA, Johnston RL, Dunn F. Comprehensive compilation of empirical ultrasonic properties of mammalian tissues. J Acoust Soc Am 1978;64:423–457.

Higdon RL. Absorbing boundary conditions for elastic waves. Geophys Soc Explor Geophys 1991;56:231–241.

Hynynen K, McDannold N, Vykhodtseva NI, Raymond S, Weissleder R, Jolesz FA, Sheikov N. Focal disruption of the blood-brain barrier due to 260-kHz ultrasound bursts: A method for molecular imaging and targeted drug delivery. J Neurosurg 2006;105:445–454.

Kaur J, Zhao Z, Klein GM, Lo EH, Buchan AM. The neurotoxicity of tissue plasminogen activator? J Cereb Blood Flow Metab 2004;24:945–963.

Kondo I, Mizushige K, Ueda T, Masugata H, Ohmori K, Matuo H. Histological observations and the process of ultrasound contrast agent enhancement of tissue plasminogen activator thrombolysis with ultrasound exposure. Jpn Circ J 1999;63:478–484.

Kornowski R, Meltzer RS, Chernine A, Vered Z, Battler A. Does external ultrasound accelerate thrombolysis? Results from a rabbit model. Circulation 1994;89:339–344.

Kudo S. Thrombolysis with ultrasound effect. Tokyo Jikeikai Med J 1989;104:1005–1012.

Lauer CG, Burge R, Tang DB, Bass BG, Gomez ER, Alving BM. Effect of ultrasound on tissue-type plasminogen activator-induced thrombolysis. Circulation 1992;86:1257–1264.

Meunier JM, Holland CK, Lindsell CJ, Shaw GJ. Duty cycle dependence of ultrasound enhanced thrombolysis in a human clot model. Ultrasound Med Biol 2007;33:576–583.

Moehring MA, Voie AH, Spencer MP, Amory DW, Alexandrov AV. Investigation of transcranial Doppler (TCD) power output for potentiation of tissue plasminogen activator (tPA) - Therapy in stroke. Cerebrovasc Dis 2000;10(Suppl. 1):9.

O'Brien WD Jr. Ultrasound-biophysics mechanisms. Prog Biophys Mol Biol 2007;93:212–255.

Pfaffenberger S, Devcic-Kuhar B, Kollmann C, Kastl C, Kaun C, Speidl WS, Weiss TW, Demyanets S, Ullrich R, Sochor H, Wober C, Zeitlhofer J, Huber K, Groschl M, Benes E, Maurer G, Wojta J, Gottsauner-Wolf M. Can commercial diagnostic ultrasound device accelerate thrombolysis? An *in vitro* skull model. Stroke 2005;36:124–128.

Press WH, Teukolsky SA, Vetterling WT, Flannery BP. Numerical Recipes in C. Cambridge: Cambridge University Press; 1992. 836–849.

Reinhard M, Hetzel A, Krüger S, Kretzer S, Talazko J, Ziyeh S, Weber J, Els T. Blood-brain barrier disruption by low-frequency ultrasound. Stroke 2006;37:1546–1548.

Shaw GJ, Bavani N, Dhamija A, Lindsell CJ. Effect of mild hypothermia on the thrombolytic efficacy of 120 kHz ultrasound enhanced thrombolysis in an in vitro human clot model. Thromb Res 2006;117:603–608.

Vykhodtseva NI, Hynynen K, Damianou C. Histologic effects of high intensity pulsed ultrasound exposure with subharmonic emission in rabbit brain *in vivo*. Ultrasound Med Biol 1995;21:969–979.

Wang Z, Moehring MA, Voie AH. *In vitro* evaluation of dual mode ultrasonic thrombolysis method for transcranial application with an occlusive thrombosis model. Ultrasound Med Biol 2008;34:96–102.

Wells PNT. Ultrasonics in medicine and biology. Phys Med Biol 1977;22:629–669. Q13